Spin-polarized transport properties of GdN nanocontacts

Ilia N. Sivkov, Oleg O. Brovko, and Valeri S. Stepanyuk
Max Planck Institute of Microstructure Physics, Halle, Germany
(Received 7 February 2014; published 14 May 2014)

Gadolinium nitride (GdN) nanocontacts were recently experimentally shown to be efficient spin filters. Our study is aimed at identifying and analyzing the physical processes responsible for the high spin polarization of the tunneling current in GdN nanostructures. By the example of planar contacts and atomic chains attached to Cu electrodes we assert, using first principle techniques, that a 100% spin-filtering effect can be indeed achieved in GdN nanocontacts. Our analysis shows that the spin filtering is due to the predominant role of nitrogen majority p states in the electron transport, while minority conductance decays exponentially with contact size due to the presence of a minority band gap at the Fermi level. Additionally, GdN zigzag infinite chains are found to be as efficient spin filters as their planar contact counterparts, also exhibiting a 100% spin-filtering effect, which is robust against chain geometry changes.

DOI: 10.1103/PhysRevB.89.195419 PACS number(s): 73.23.−b, 75.50.Pp, 73.63.Rt, 72.25.−b

I. INTRODUCTION

The explosive increase in interest of both science and technology in spin-based electronic devices creates a high demand in spin-polarized electron sources. While in spectroscopical applications the spin filtration can be achieved by free electron scattering from a magnetic or strong-spin-orbit-coupling surfaces [1], for integrated spin circuitry one has to resort to "spin-filtering" materials or structures for creation and injection of spin-polarized currents [2,3]. First studies of the spin-polarized current were related to the work of Meservey and Tedrow [4], where spin-polarized electrons were injected from a ferromagnetic metal into a nonmagnetic material. In further studies spin-polarized currents were investigated in ferromagnetic-metal/insulator/ferromagnetic-metal junctions, which eventually led to the development of realistic memory devices [5,6]. A large number of studies dealt with spin-polarized transport phenomena in semiconductors [7–14], mainly concentrating on Eu-based compounds. In particular, EuO films were shown to cause a 100% spin polarization of the current [9,12,14].

In recent years, however, another interesting compound—GdN—started to draw attention to itself. GdN is comprised of a ferromagnetically coupled Gd sublattice to which N atoms are antiferromagnetically coupled. The moment per unit cell is as high as $7\mu_B$. But most importantly, GdN has a half-metallic electronic structure [15–19]. Its minority electronic structure has a gap at the Fermi level and behaves like a semiconductor, while majority channel has a semimetal electronic structure. The possibility of utilizing the half-metallicity of GdN for spin filtering was suggested in Ref. [16]. It was also shown that this feature of the crystal depends on the lattice constant. In recent works [20–22] transport properties of GdN films were investigated experimentally. Ludbrook and co-workers [20] were able to achieve a tunneling magnetoresistance ratio (TMR) of 35%. Later, Pal *et al.* and Senapati *et al.* [21,22] reported observing a spin polarization of conductance reaching 90% in a GdN film sandwiched between NbN electrodes.

In the present paper we study transport properties of GdN(001) films and GdN diatomic wires attached to Cu(001) electrodes with *ab initio* means. We show that the spin polarization of conductance can indeed reach 100% in both systems and give detailed explanation of the spin-filtering mechanism in terms of electronic structure of the compound. We also expand our study onto the case of GdN chains, which show equally excellent spin-filtering properties, which are robust against chain-geometry changes.

II. METHOD

For the calculation of the self-consistent electronic structure and geometry of the systems SIESTA code was used [23,24], which implements density functional theory (DFT) on the Kohn-Sham level of abstraction, and uses linear combination of atomic orbitals (LCAO) for basis sets and Troullier-Martins norm-conserving pseudopotentials for atomic core treatment [25]. Both pseudopotentials and the calculation formalism are scalar relativistic and spin polarized. Transport calculations were performed in the SMEAGOL code [26,27], which is based on SIESTA and utilizes nonequilibrium Green's functions (NEGF) to obtain the conductance of the system in the framework of the Landauer-Büttiker transport formalism.

As a LCAO basis set for the Gd, $6s$ double-ζ and $6p,5d,4f$ single-ζ basis states were chosen. Basis for the N consisted of $2s,2p$ double-ζ and $3d$ single-ζ basis states. For the Cu we chose the basis states to include $4s,3d$ double-ζ and $4p$ single-ζ.

For the exchange-correlation functional we chose the GGA approximation, since it is known to be more accurate in the description of the electronic structure. In the particular case of GdN, GGA yields a gap of 0.68 eV in the minority channel, which is in good agreement with previous studies [15–19]. At the same time, LDA approximation, e.g., predicts the electronic structure to be metallic in both spin channels.

Since Gd is an f element, it's important to account for the strong on-site correlation of the f shell. To this end, GGA+U approximation was utilized with $U = 6.7$ and $J = 0.7$ as per Ref. [28], where these parameters were calculated from first principles.

III. RESULTS

A. GdN film contact

As a model system of a planar GdN junction we consider an fcc (001) slab of GdN sandwiched between two Cu(001)

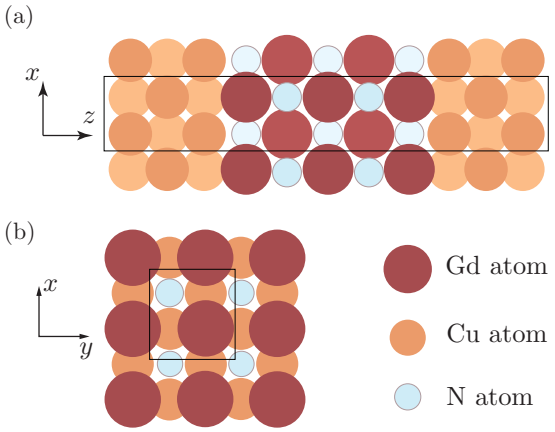

FIG. 1. (Color online) (a) Sketch of the studied system—a Cu/GdN/Cu planar nanocontact. (b) Top view of the last Cu layer and the first GdN layer at the Cu/GdN interface. Black frames denote one unit cell, used for calculation.

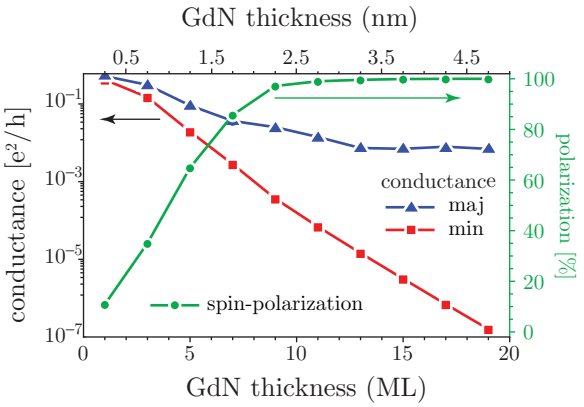

FIG. 2. (Color online) Majority (blue triangles) and minority (red squares) zero-bias conductance of a Cu/GdN/Cu tunneling junction at the Fermi level (logarithmic scale) and the resulting polarization of conductance (green circles) as a function of GdN-layer thickness.

electrodes, that act as leads for electron transport (see Fig. 1). A calculation (GGA+U) of GdN bulk yields an equilibrium lattice constant 5.027 Å. The length of face diagonal of Cu(001) is $a_{Cu}\sqrt{2} = 5.191$ Å, which amounts to a mismatch of about 5%, which is within reasonable margins for epitaxial growth. This makes an epitaxial growth of GdN at a 45° to Cu(001) lattice the most likely scenario. To simulate this, the lattice constant of GdN was compressed to match that of Cu fcc face diagonal. A number of layers in the GdN slab varied from 1 to 19 in bilayer steps. The interlayer distances of GdN were allowed to relax freely, thus simulating the case when GdN is grown epitaxially in Cu(001) and subsequently capped again by Cu to form a contact junction. In the following we shall assume that the interface lies in the xy plane and the electron transport takes place along the z direction. Before we proceed to the discussion of obtained results, we shortly note that Liu *et al.* [29] have recently reported that strained GdN bulk systems can exhibit ferroelectric behavior at strain values of as low as 3%. While the finding does not affect the conclusions of the present paper (the authors report that within a broad strain range the ground state magnetic properties are robust or altogether unaffected) the idea of the possibility of ferroelectricity in epitaxially grown GdN makes the system even more attractive for further studies, both fundamental and applied [29].

Figure 2 shows the zero-bias conductance of a Cu/GdN/Cu nanojunction as a function of GdN layer thickness. The conductance is split into majority and minority electron contributions (blue triangles and red squares, respectively) and is given in logarithmic scale. The spin polarization of conductance, calculated as $P = (G_\uparrow - G_\downarrow)/(G_\uparrow + G_\downarrow) \times 100\%$ (where $G_\uparrow$ and $G_\downarrow$ are the conductance values in spin-up and spin-down channels, respectively) is plotted in green circles with a corresponding axis on the right. It can be seen that with increasing the number of layers the total conductance decreases. The noteworthy fact is, however, that while minority conductance shows a continuous exponential decay with thickness (linear behavior in log scale), majority conductance "saturates" at $0.007e^2/h$ when the thickness of GdN exceeds ~13–15 layers. Therefore, the difference in the conductances between spin-up and spin-down channels gradually increases, reaching several orders of magnitude and causing the spin polarization of conductance to approach 100%.

In general, the GdN-thickness dependence of conductance can be expected to have two distinctly different behavior ranges. For thinner slabs, the transport shall be determined mostly by the interface effects, while for thicker slabs the tunneling can be expected to approach slab-GdN characteristics. Judging from the curves in Fig. 2, for GdN the boundary between those two regimes can be drawn at about 13–15 layers. We shall attempt to understand the electronic properties responsible for the conductance characteristics in both regimes.

Since we are interested in GdN's impressive spin-filtering ability we shall start from analyzing the bulklike conductance, which is observed for thicker GdN slabs. Even without having a detailed knowledge of the electronic structure of GdN, but only from analyzing the thickness dependence of conductance (Fig. 2) we can surmise that the exponential decay of zero-bias minority conductance is caused by a gap at the Fermi level, while constant majority conductance is a hint that conductance channels exist in GdN bulk for majority electrons around E_F. To verify that surmise we take a look at symmetry decomposed projected density of states (PDOS) of GdN bulk. In Fig. 3 the LDOS of p_x, p_y, p_z states of N and d_{xy}, d_{xz}, d_{yz} of Gd are shown. The densities of states of other orbitals are too small to be discernible at the scale of the graph and are thus omitted, as they are unlikely to significantly contribute to the transport. As it was mentioned, GdN and Cu lattices have a mismatch of about 5%; thus GdN/Cu is strained in the plane of the interface. This distortion has an effect of raising the degeneracy between of p_x, p_y, and p_z states of N [green dotted and solid red curves in Fig. 3(a), respectively] and d_{xy} and d_{xz}, d_{yz} states of Gd [green dotted and solid red curves in Fig. 3(b), respectively]. Corresponding p and d states of N and Gd in bulk GdN are degenerate and are shown with shaded areas in Figs. 3(a) and 3(b).

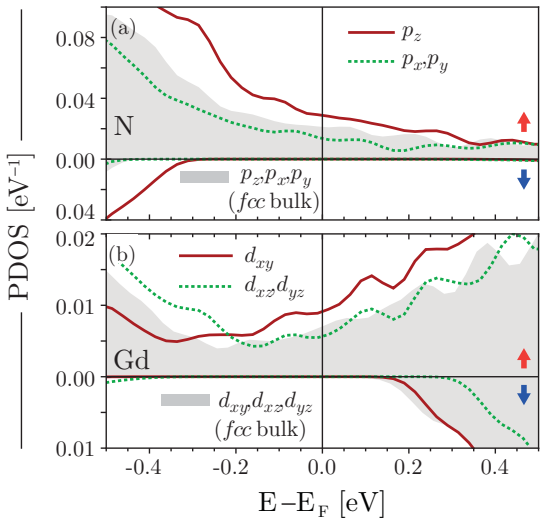

FIG. 3. (Color online) Spin resolved projected density of states of N-p_x, p_y, p_z (a) and Gd-d_{xy}, d_{xz}, d_{yz} (b) states for an infinitely thick slab of GdN epitaxially sandwiched between Cu electrodes (stretched in the xy plane by 5% and allowed to relax along the z direction; see text for discussion). Shaded areas present the corresponding DOS of an ideal GdN bulk.

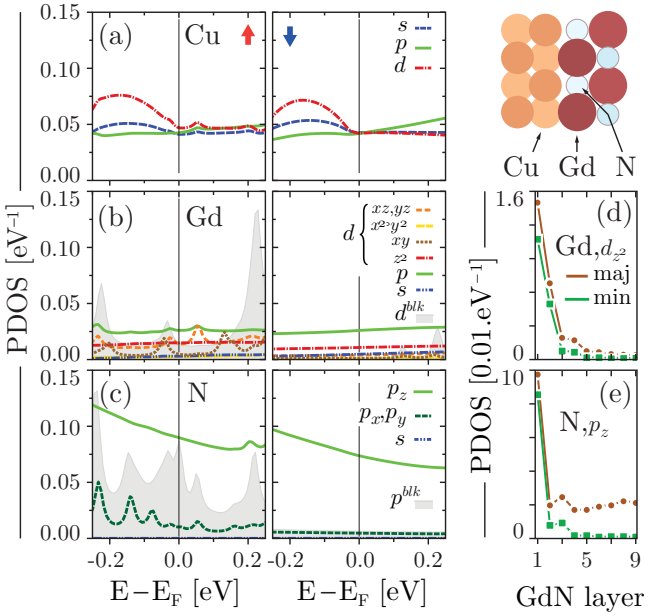

FIG. 4. (Color online) Symmetry decomposed PDOS of the interface Cu (a), Gd (b). and N (c) atoms of a Cu/GdN/Cu junction with 19 GdN layers. Shaded areas in (b) and (c) represent the Gd-d_{tot} and N-p_{tot} PDOS of the central layer of the junction, which is nigh-identical to bulk GdN. Layer resolved Fermi level PDOS of Gd-d_{z^2} and N-p_z states is shown in (d) and (e), respectively.

The most obvious feature in Fig. 3 is the gap in minority LDOS ranging from −0.3 to 0.2 eV, which inhibits electron transport. The transmission of minority electrons through GdN can thus be described as a Wentzel-Kramers-Brillouin-like (WKB) problem of electrons tunneling through a rectangular barrier [30]. In accordance with that we observe an exponential decay in minority conductance with increasing GdN thickness (Fig. 2). Majority LDOS of GdN is relatively flat and featureless around the Fermi level, forming a conduction band and enabling resonant ballistic transport. The main contributors here are p_z and d_z states, since they have the highest densities and are oriented along the transport direction.

It must be noted, however, that even at large thicknesses of GdN the conductance is not determined solely by the bulk-like-GdN band structure, but also by the electron injection from Cu into GdN, which is in turn determined by the hybridization and band alignment at the interface. This hybridization is even more important for electron transport through thin GdN layers, since then it becomes the main factor determining the transmission properties of the junction. To understand the electronic structure of the interface we plot in Figs. 4(a)–4(c) the symmetry decomposed projected density of states of the interface Cu, Gd, and N atoms (particular atoms are marked with arrows in the inset) of a Cu/GdN/Cu junction with a 19-layer-thick GdN slab. Cu atoms at the interface have a relatively flat LDOS around the Fermi level with comparable densities of s, p, and d electrons, providing a good basis for hybridization with GdN. Gd atoms at the interface, similar to the bulk ones, have a fairly low density of states around the Fermi level. Compared to bulk (gray shaded area in Fig. 4 [31]) the d states of interface Gd are slightly shifted, due to a mild hybridization with Cu. However, only majority d_{z^2}, $d_{xz,yz}$, and $d_{x^2-y^2}$ are nonvanishing, and even they have a fairly small density, only weakly contributing to the conduction through the interface. The p states, on the contrary, are nonzero in both spin channels (while their density in bulk is almost zero at the Fermi level) due to hybridization with Cu atoms. In particular, p-PDOS (mainly p_z, as could be expected) exceeds the density of d states in both spin channels, thus contributing to conductance, but reducing the spin polarization thereof. The main hybridization effect, however, can be traced in the density of p states of interface N atoms. Even in GdN bulk, minority p-LDOS is the dominant contribution at the Fermi level. At the interface not only is the majority p_z LDOS greatly enhanced, but in the minority p_z are filled by the overlap with Cu states. Thus N-p states exceed by almost an order of magnitude the density of any other GdN state at the interface. This efficient hybridization of both majority and minority p states of N with Cu determine the conductance at the interface, drastically reducing its spin polarization for thin GdN junctions.

To see how deep into GdN the hybridization goes we plot in Figs. 4(d) and 4(e) the value of the spin-resolved local density of states at E_F of the dominant hybridized orbitals (N-p_z and Gd-d_{z^2} are shown as representative examples) for different layers of GdN. High at the interface due to hybridization with Cu, both N-p_z and Gd-d_{z^2} LDOS decay as one goes deeper into the GdN slab, achieving their respective equilibrium bulk values by about the fifth layer. Thus the "direct" electron injection length from Cu into GdN can be estimated to be about 10–15 Å. For a system with comparable GdN layer thickness the transport shall be determined by the interface properties, rather than by the properties of GdN bulk. A careful examination of conductance behavior with GdN thickness (shown in Fig. 2) will reveal at a thickness of about 10 layers

(twice 5) a small bend in the exponential decay of the minority and a saturation of majority conductances.

At the end of this section one can summarize that GdN films between Cu electrodes exhibit spin-filtering properties due to differences in majority and minority electron tunneling, resulting in spin polarization of conductance reaching 100%. At the Cu/GdN interface, electrons are injected from Cu primarily into p states of N and d_{z^2} and p_z states of Gd. At GdN thicknesses exceeding 5–10 monolayers the gap opens in the minority LDOS, leading to an exponential decay of minority-channel conductance. The tunneling of majority electrons carries a resonant character (based on the GdN bulk electronic levels/bands) and saturates at GdN thicknesses over 10–15 monolayers. At those thicknesses the spin polarization of conductance reaches 100%, producing a nigh-perfect spin-filtering junction.

B. Infinite Gd-N chain

At present, many studies are aiming at nanospintronic applications, in particular those dealing with electronic and transport properties of low-dimensional nanoscale systems, such as atomic chains or clusters [32–40]. Understanding the behavior of such systems can give an impulse for creating fundamentally new data storage and processing devices. Knowing the excellent spin-filtering properties of planar GdN junctions it is only logical to ask oneself whether GdN nanocontacts, in particular nanochains, share the same property.

We performed transport calculations for a planar infinite zigzag GdN chain. The chain was constructed of alternating Gd and N atoms ordered in a zigzag or linear fashion along the z axis (Fig. 5). Calculations were performed for different distances between neighboring Gd atoms d. The N atoms were always allowed to assume equilibrium positions by fully relaxing the system. The only constraint imposed was the requirement for the system to stay planar in the yz plane. In this manner, electronic structure and transport properties were obtained for differently stretched GdN chains.

Energy of the chain and equilibrium width h (extent of the zigzag along the y axis) are presented in Fig. 5(a) (black circles and gray rectangles, respectively). The chain has a global energy minimum at $d = 3.8$ Å, which corresponds to a zigzag structure with parameter $h = 1.2$ Å. Transition to a linear structure is rather sharp and occurs after a small energetic barrier at about $d = 4.2$ Å.

The coupling between Gd atoms was found to be ferromagnetic regardless of the stretching parameter d, while N atoms were always coupled antiferromagnetically to Gd. Such GdN magnetic structure coincides with the bulk one. Magnetic moments of N and Gd in the chain are slightly larger than they are in the bulk ($0.75\mu_B$ and $7.75\mu_B$ vs $0.25\mu_B$ and $7.25\mu_B$, respectively), and remain constant practically in the whole studied range of d (from 3.2 to 4.4 Å). The chain, similar to the GdN bulk, has a gap in minority DOS around the Fermi level for all studied stretching parameters d. The filled minority band is not affected by stretching, which results in the magnetic moment of the whole system staying constant at ($7.0\mu_B$) during stretching. Despite the changes in geometry of the zigzag chain, stretching-induced charge transfer within the chain is small, keeping partial magnetic moments of Gd and N constant.

The spin-resolved conductance and its resulting spin polarization are presented in Figs. 5(b) and 5(c), respectively. In agreement with the gap in minority DOS, the minority channel has zero conductance practically in the whole studied

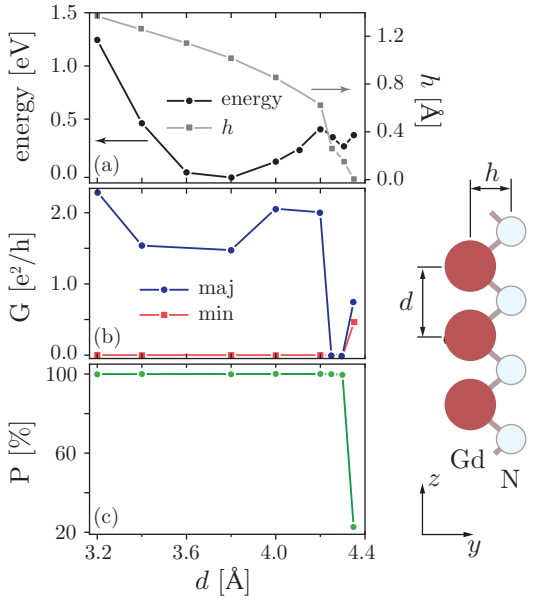

FIG. 5. (Color online) Energy and equilibrium parameter h (a), spin resolved zero-bias conductance (b), and spin polarization of conductance (c) of a planar GdN chain (sketch on the right) as a function of the chain stretching parameter d.

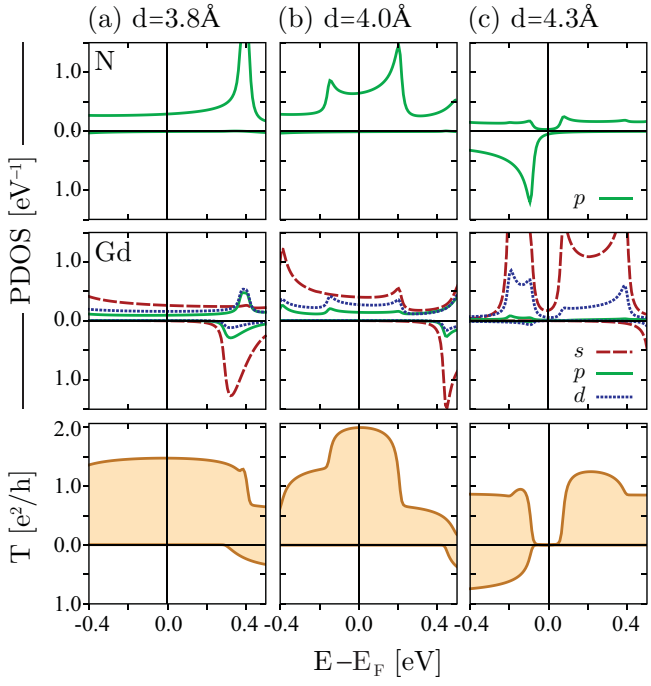

FIG. 6. (Color online) Projected density of states (top panels: N-p; middle: Gd-s,p,d) and zero-bias transmission coefficients (bottom panels) of infinite Gd-N chain at stretching parameters d of 3.8 (a), 4.0 (b), and 4.3 Å (c).

stretching range, which results in a 100% spin- polarization of conductance, making a GdN chain as good a spin filter as the planar GdN junctions are. There is, however, one intriguing feature in conduction at $d = 4.3$ Å. This configuration corresponds to a linear chain and displays an insulating behavior in both spin channels suppressing conductance altogether [Fig. 5(b)]. While this feature might have been of interest to technological applications, $d = 4.3$ Å is also very close to the point of structural instability of the chain and thus we shall leave its detailed discussion to be a matter of future studies.

Analysis of the projected density of states of Gd and N has shown that the conductance of majority electrons is mostly contributed to by the hybridization of N-p and Gd-s,d states [plotted in Fig. 6(upper and middle panels)] for $d = 3.8$, 4.0, and 4.3 Å [Figs. 6(a), 6(b), and 6(c), respectively]. The N-p states are mainly represented by p_y, p_z symmetries, reflecting the geometry of the chain lying in the yz plain. Gd d states are mostly represented by d_{z^2}, d_{yz}, and $d_{x^2-y^2}$ states. A narrow majority PDOS peak at 0.4 eV for a chain of $d = 3.8$ Å (which is in fact a narrow band) moves towards the Fermi level and expands during the stretching of the chain to $d = 4.0$ Å forming an additional conductance channel. This explains the increase of majority-spin conduction, as can be observed in Fig. 5(b). The shift of that peak can also explain the observed insulating behavior at $d = 4.3$ Å. As the chain is stretched from 4.0 to 4.3 Å the above-mentioned band shifts away from the Fermi level leaving it devoid of conductance channels [Fig. 6(c)].

IV. CONCLUSIONS

To summarize, both planar and chainlike GdN junctions have excellent spin-filtering properties, which are caused by the energy gap in minority DOS at the Fermi level.

For thick planar Cu/GdN/Cu junctions (over 10–15 layers of GdN) the conductance is determined by the bulklike properties of GdN. The minority gap and resonant ballistic conductance in the the majority channel ensure 100% spin polarization of the small-bias tunneling current. For thinner GdN slabs the conductance is determined by the hybridization at the interfaces and the injection of electrons from Cu into GdN. Since both majority and minority electrons are injected alike, the spin filtering in thin junctions is somewhat less efficient.

Zigzag infinite GdN chains as well exhibit 100% spin-polarized conductance in a wide stretching range due to a large gap in minority DOS. It is conceivable that such chains, freely suspended or, more likely, adsorbed on an insulating layer, could find application as spin filters in nanospintronic devices.

[1] J. Kirschner, D. Rebenstorff, and H. Ibach, Phys. Rev. Lett. **53**, 698 (1984).

[2] J. S. Moodera, G.-X. Miao, and T. S. Santos, Phys. Today **63**, 46 (2010).

[3] I. Žutić and S. Das Sarma, Rev. Mod. Phys. **76**, 323 (2004).

[4] P. Tedrow and R. Meservey, Phys. Rev. Lett. **26**, 192 (1971).

[5] M. Julliere, Phys. Lett. A **54**, 225 (1975).

[6] S. Parkin, C. Kaiser, A. Panchula, K. Roche, and M. Samant, Proc. IEEE **91**, 661 (2003).

[7] V. V. Osipov, N. A. Viglin, V. I. Kochev, and A. A. Samokhvalov, JETP Lett. **52**, 386 (1990).

[8] V. Osipov, N. Viglin, and A. Samokhvalov, Phys. Lett. A **247**, 353 (1998).

[9] T. S. Santos and J. S. Moodera, Phys. Rev. B **69**, 241203(R) (2004).

[10] P. G. Steeneken, L. H. Tjeng, I. Elfimov, G. A. Sawatzky, G. Ghiringhelli, N. B. Brookes, and D.-J. Huang, Phys. Rev. Lett. **88**, 047201 (2002).

[11] M. Müller, G.-X. Miao, and J. S. Moodera, Europhys. Lett. **88**, 47006 (2009).

[12] P. V. Lukashev, A. L. Wysocki, J. P. Velev, M. van Schilfgaarde, S. S. Jaswal, K. D. Belashchenko, and E. Y. Tsymbal, Phys. Rev. B **85**, 224414 (2012).

[13] P. V. Lukashev, J. D. Burton, A. Smogunov, J. P. Velev, and E. Y. Tsymbal, Phys. Rev. B **88**, 134430 (2013).

[14] N. Jutong, I. Rungger, C. Schuster, U. Eckern, S. Sanvito, and U. Schwingenschlögl, Phys. Rev. B **86**, 205310 (2012).

[15] C. Mitra and W. R. L. Lambrecht, Phys. Rev. B **78**, 134421 (2008).

[16] C.-g. Duan, R. F. Sabiryanov, J. Liu, W. N. Mei, P. A. Dowben, and J. R. Hardy, Phys. Rev. Lett. **94**, 237201 (2005).

[17] P. Larson and W. R. L. Lambrecht, Phys. Rev. B **74**, 085108 (2006).

[18] C. M. Aerts, P. Strange, M. Horne, W. M. Temmerman, Z. Szotek, and A. Svane, Phys. Rev. B **69**, 045115 (2004).

[19] A. G. Petukhov, W. R. L. Lambrecht, and B. Segall, Phys. Rev. B **53**, 4324 (1996).

[20] B. M. Ludbrook, I. L. Farrell, M. Kuebel, B. J. Ruck, A. R. H. Preston, H. J. Trodahl, L. Ranno, R. J. Reeves, and S. M. Durbin, J. Appl. Phys. **106**, 063910 (2009).

[21] A. Pal, K. Senapati, Z. H. Barber, and M. G. Blamire, Adv. Mater. **25**, 5581 (2013).

[22] K. Senapati, M. G. Blamire, and Z. H. Barber, Nat. Mater. **10**, 849 (2011).

[23] P. Ordejón, E. Artacho, and J. M. Soler, Phys. Rev. B **53**, R10441 (1996).

[24] J. M. Soler, E. Artacho, J. D. Gale, A. García, J. Junquera, P. Ordejón, and D. Sánchez-Portal, J. Phys.: Condens. Matter **14**, 2745 (2002).

[25] N. Troullier and J. L. Martins, Phys. Rev. B **43**, 1993 (1991).

[26] A. R. Rocha, V. M. García-Suárez, S. W. Bailey, C. J. Lambert, J. Ferrer, and S. Sanvito, Nat. Mater. **4**, 335 (2005).

[27] A. R. Rocha, V. M. García-Suárez, S. W. Bailey, C. J. Lambert, J. Ferrer, and S. Sanvito, Phys. Rev. B **73**, 085414 (2006).

[28] B. Harmon, V. Antropov, A. Liechtenstein, I. Solovyev, and V. Anisimov, J. Phys. Chem. Solids **56**, 1521 (1995).

[29] H. M. Liu, C. Y. Ma, C. Zhu, and J.-M. Liu, J. Phys.: Condens. Matter **23**, 245901 (2011).

[30] B. M. Karnakov and V. P. Krainov, *WKB Approximation in Atomic Physics* (Springer, Berlin, 2013), p. 176.

[31] In fact, the shaded area represents the *d* LDOS of the central atom of the 19-atom slab and slightly deviates from the true bulk density shown in Fig. 3, exhibiting several peaks, which we ascribe the formation of quantum well states in the finite-thickness GdN slab. The same holds for the appearance of similar peaks in the $p_{x,y}$ density of states of N [see shaded area in Fig. 4(c)].

[32] K. Tao, I. Rungger, S. Sanvito, and V. S. Stepanyuk, Phys. Rev. B **82**, 085412 (2010).

[33] K. Tao, V. S. Stepanyuk, W. Hergert, I. Rungger, S. Sanvito, and P. Bruno, Phys. Rev. Lett. **103**, 057202 (2009).

[34] L. Vitali, R. Ohmann, S. Stepanow, P. Gambardella, K. Tao, R. Huang, V. S. Stepanyuk, P. Bruno, and K. Kern, Phys. Rev. Lett. **101**, 216802 (2008).

[35] K. Tao, V. S. Stepanyuk, P. Bruno, D. I. Bazhanov, V. V. Maslyuk, M. Brandbyge, and I. Mertig, Phys. Rev. B **78**, 014426 (2008).

[36] A. Bernand-Mantel, P. Seneor, N. Lidgi, M. Muñoz, V. Cros, S. Fusil, K. Bouzehouane, C. Deranlot, A. Vaures, F. Petroff, and A. Fert, Appl. Phys. Lett. **89**, 062502 (2006).

[37] N. Néel, J. Kröger, and R. Berndt, Phys. Rev. Lett. **102**, 086805 (2009).

[38] N. Néel, J. Kröger, and R. Berndt, Phys. Rev. B **82**, 233401 (2010).

[39] C. Lazo, N. Néel, J. Kröger, R. Berndt, and S. Heinze, Phys. Rev. B **86**, 180406 (2012).

[40] N. Néel, S. Schröder, N. Ruppelt, P. Ferriani, J. Kröger, R. Berndt, and S. Heinze, Phys. Rev. Lett. **110**, 037202 (2013).